

Porous Carbon Networks with Nanosphere-Interconnected Structure *via* 3-Aminophenol-Formaldehyde Polymerization

Deul Kim^{†,1}
 Seokjin Yun^{†,1}
 Sangeun Chun^{*,2}
 Jihoon Choi^{*,1}

¹ Department of Materials Science and Engineering, Chungnam National University,

Daejeon 34134, Korea

² Department of Materials Science and Engineering, Kyungpook National University,

Daegu 41566, Korea

Received June 21, 2017 / Revised November 20, 2017 / Accepted November 27, 2017

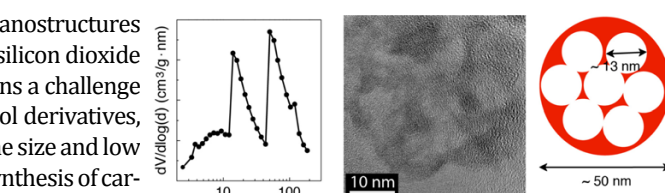
Abstract: Although mesoporous carbon materials with hierarchical nanostructures have been produced by the synthesis of hybrid nanoparticles with a silicon dioxide (SiO_2) core and a shell of resorcinol formaldehyde resin, it still remains a challenge to effectively tune the pore size distribution. Among a series of phenol derivatives, 3-aminophenol was found to exhibit not only excellent tunability of the size and low roughness of the sphere surface but also high pyrolysis yields in the synthesis of carbon nano/microspheres. Here, we report that mesoporous carbon networks with a bimodal pore size distribution in their hierarchical nanostructure were prepared by 3-aminophenol and formaldehyde polymerization on the SiO_2 cores. In particular, the systematic control of the ratio of carbon precursors and silica nanoparticles provides a better control of the microstructure in hybrid nanoparticles with a shell of variable thickness composed of well-defined 3-aminophenol and formaldehyde resins, resulting in the tunability of their pore size distribution.

Keywords: 3-aminophenol, porous carbon, hollow carbon sphere, interconnected carbon.

1. Introduction

Common usage of porous carbon materials in the fields of catalysis, adsorption, electronics, and energy conversion/storage highly depends on their nanostructures such as pore size, pore distribution, and shell thickness.^{1–5} Due to their critical role in the material performance, many efforts have been invested in developing a suitable design and controlled fabrication of nanoporous organic polymers and carbon materials to achieve a wide variety of well-defined nanostructures such as ordered/disordered mesoporous/macroporous carbons, hollow carbon spheres, and hierarchical porous carbons.^{5–9} In particular, hard or soft templating methods based on the incompatibility between the templates and carbon precursors are the most popular and effective to control the nanoporous structures defined by the size and shape as well as the volume ratio of the templates.^{6–11} For example, Schuster *et al.* demonstrated the nitrogen-doped porous hollow carbon spheres for improving lithium-sulfur batteries using hard templates (*i.e.* silica nanoparticles) and Liu *et al.* reported mesoporous (~3.5 nm) carbon nanospheres with particle size from 80 to 400 nm using soft templates such as cationic fluorocarbon surfactant and triblock copolymer.^{9,10}

Phenolic resins have been widely used as carbon precursor



for the synthesis of various nanostructured carbon materials due to their thermal stability, high carbon yield and versatile chemical properties in various applications such as adsorbents, supercapacitors, and lithium-ion battery electrodes.^{12–14} For example, Pekala reported that the polycondensation of resorcinol with formaldehyde results in the cross-linking of their clusters (*i.e.* resorcinol-formaldehyde gel; RF), which was further used as carbon precursors.¹⁵ In addition, the RF polymerization mechanism was shown to be similar to the sol-gel processing of silica where silica sphere or network is preferentially formed depending on the acid or base condition.^{16,17} Recently, Stöber method was extended to prepare monodisperse RF resin particles where carbon spheres were obtained by a simple carbonization of the resin spheres.¹⁵ However, a precise control of the surface properties of the resultant polymer resin spheres is a still challenge due to the high concentration of the RF precursor used in the synthesizing process. For instance, Han *et al.* reported a facile route to fabricate nanoporous carbons by resorcinol-formaldehyde polymerization in the presence of silica nanoparticles and subsequent carbonization and silica etching.¹⁸ However, in this approach the pore size distribution (*i.e.* about 10~100 nm) is not well controlled due to insufficient coating of resorcinols onto the individual silica nanoparticles of aggregates.

Recently, Zhao *et al.* investigated a series of phenol derivatives such as 2-aminophenol, 3-aminophenol, 4-aminophenol, 3-methylphenol, and 1,3,5-trihydroxybenzene for the synthesis of monodisperse resin and carbon nanospheres through hydrolysis and condensation in the basic condition.¹⁹ Among these candidates, 3-aminophenol-formaldehyde (3-AF) resin

Acknowledgment: This work is supported by the National Research Foundation of Korea (NRF) grant funded by the Korean government (No. NRF-2015R1C1A1A01052865).

***Corresponding Authors:** Sangeun Chun (sangeun@knu.ac.kr), Jihoon Choi (jihoonc@cnu.ac.kr)

[†]These authors contributed equally to the presented work.

was shown to provide the size tunability of nanospheres as well as significantly reduced roughness of the particle surfaces.^{14,19,20}

In this work, we demonstrate the porous carbon networks with controlled pore sizes in a nanosphere-interconnected structure by replacing a resorcinol (with two hydroxyl groups) with 3-aminophenol (with a hydroxyl and an amine group) as carbon precursor. In particular, amine groups of 3-AFs would show more preferential attraction with the hydroxyl groups on the surface of the silica nanoparticles compared to hydroxyl groups of RFs, leading to more uniform coatings of resin on the individual silica nanoparticles of aggregates. A network of 3-AF resin allows the formation of the nanosphere-interconnected structure that results in the hierarchical nanostructure with pore sizes of ~13 nm and ~50 nm in porous carbon networks, providing a route to strategically design the porous carbon materials with a controlled nanostructure.

2. Experimental

2.1. Materials

SiO_2 nanoparticles (~13 nm) were obtained from Sigma-Aldrich (Ludox, ~30 wt%). 3-aminophenol (>98%) and formaldehyde (35~38 wt%) were purchased from Alfa Aesar and Daejung Chemicals & Metals Co., Ltd, respectively. Anhydrous ethanol and ammonium solution ($\text{NH}_3\text{H}_2\text{O}$) (25%) were purchased from Samchun Chemical. All chemicals were used as received.

2.2. Synthesis of porous carbon networks

Core-shell silica nanosphere composites were synthesized as follows : Silica nanoparticles (20 mL) were dispersed in a mixed solvent of deionized water (200 mL) and ethanol (100 mL) and sonicated for 3 h. Subsequently, 3-aminophenol was added into the silica suspension to make a certain molar ratio of 3-aminophenol to silica (1:5, 1:10, and 1:50) that were denoted as PoC-1, PoC-2, and PoC-3, respectively, and kept stirring (Figure 1). To adjust the pH (~10) a small amount of ammonium solution was added, and then a certain amount of formaldehyde solution was added to the reaction mixture, in which the mole ratio between 3-aminophenol and formaldehyde was fixed at 1:1.4. The mixture was continuously stirred overnight at room tem-

perature. The brown precipitates were removed by centrifuge, and the supernatant was dried and washed three times with deionized water and once with ethanol. 3-AF-coated silica nanoparticles were obtained by drying under vacuum at 80 °C for 5 h. The resulting sample was heated in a quartz tube to 800 °C at a rate of 5 °C/min in Ar atmosphere, kept for 8 h at this temperature. Finally, porous carbon materials were obtained by etching the resulting carbon-coated silica nanoparticles with HF, and then drying at 80 °C overnight.

2.3. Characterization

Transmission electron microscopy (TEM) images were obtained using a JEM 2100 electron microscope operated at 200 kV. Scanning electron microscopy (SEM) images were taken using a Hitachi S-4800. Fourier transform infrared spectroscopy (FTIR) spectrum (500-3500 cm^{-1}) was measured using a Bruker ALPHA-P in the transmission mode. Raman scattering spectrum (1000-2000 cm^{-1}) measurement was performed using a Horiba LabRAM HR-800 with an Ar ion laser. UV-vis absorption spectra were obtained using a Shimadzu UV-2600 spectrophotometer. Nitrogen adsorption-desorption isotherms were carried out at 77 K using a BELSORP-max analyzer. The specific surface area was calculated by the Braunauer-Emmett-Teller (BET) method. Thermogravimetric analysis (TGA) was carried out under N_2 atmosphere at a heating rate of 5 °C/min using a Mettler-Toledo TGA/DSC1.

3. Results and discussion

Carbonization of 3-AF-coated silica nanoparticles and the removal of silica cores was investigated using a FTIR as shown in Figure 2. The narrow absorption peaks (1050 and 850 cm^{-1}) owing to Si-O-Si covalent bondings completely disappear after HF etching, confirming the removal of silica cores. For the samples with higher amounts of 3-AF compared to the silica templates (PoC-1 and PoC-2), aliphatic and aromatic C-H bonds are dominantly present while PoC-3 exhibits more significant absorbance peaks corresponding to functionalized carbons (C-OH and C-H). This result can be understood as a consequence of the thinner carbon layers with higher surface areas, which results in functionalized carbon materials by harsh chemical environments during the procedure for silica etching. Characteristics on the mor-

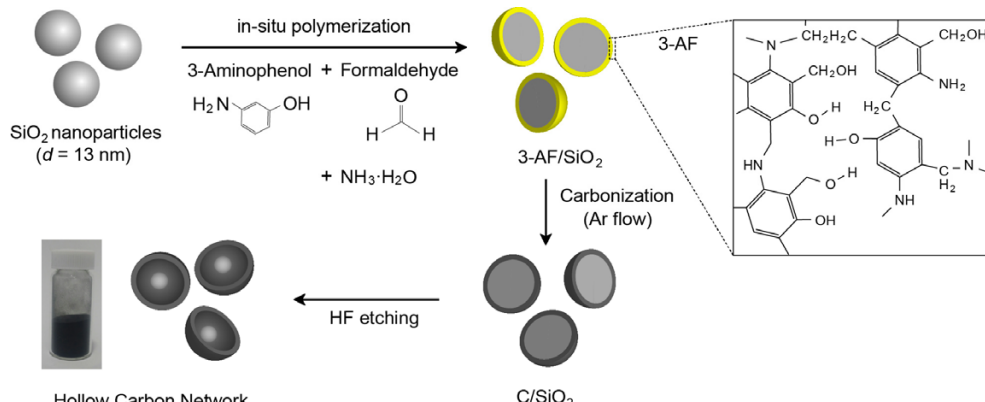


Figure 1. Preparation procedure of the formation of porous carbon networks.

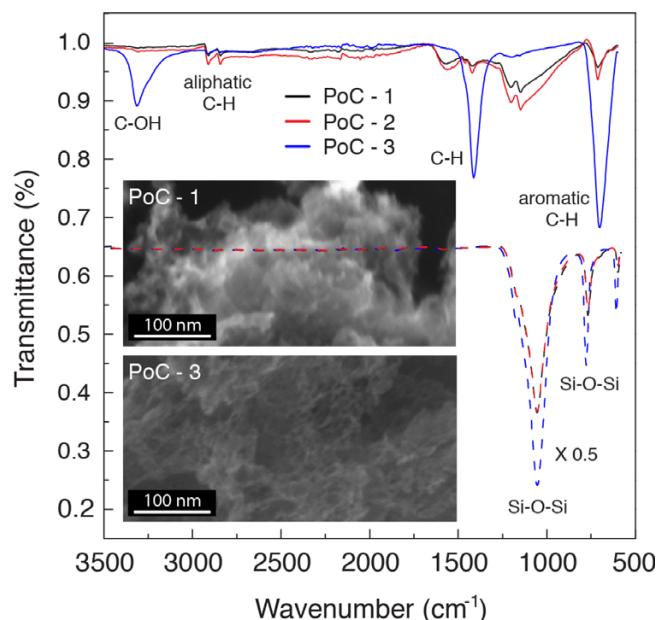


Figure 2. FTIR spectra of PoC-1, PoC-2, and PoC-3 before (dashed lines) and after (solid lines) removal of silica core nanoparticles. Insets show corresponding SEM images after silica etching.

phology of the porous carbon microstructure (PoC-1 and PoC-3) confirms the above FTIR results as shown in the SEM images (Figure 2, insets). PoC-3 exhibits an interconnected network morphology of thin carbon layers with a uniform pore size while PoC-1 shows an ill-defined microstructure due to non-uniform dispersion of silica nanoparticles and 3-AF.

Figure 3(a) and 3(b) depict transmission electron images of the neat silica nanoparticles with an average diameter of ~ 13 nm used as hard template. After a series of process including 3-AF coating, carbonization, and HF etching, the porous carbon networks were obtained as shown in Figure 3(c)-(h), revealing the dependence of their characteristic structures on the molar ratio of 3-aminophenol to silica. At low ratio, a broad distribution of pore sizes is observed in the ranges of 20~100 nm and their shape and structure is not well defined as shown in Figure 3(c) and 3(d). These irregularly shaped mesopores could be associated with the formation of the 3-aminophenol-formaldehyde gel in the presence of the aggregation of silica nanoparticles. Zhao *et al.* reported that the formation of 3-AF resin nanospheres was not observed when the concentrations of 3-aminophenol are much less than 3.27 mmol/L since no emulsion droplets were formed at the precursor concentration less than critical micelle concentration (CMC).¹⁹ In this work, the concentration of 3-aminophenol was kept much lower (about 8×10^{-6} – 8×10^{-5} mmol/L) than the CMC, and thus no 3-AF resin nanospheres were observed. Rather, 3-AF resin will induce a gel layer formation on the surface of the aggregates as well as free 3-AF gels during the reaction. This is consistent with the previous observation for porous carbon materials prepared by RF resin with silica templates.¹⁸ As the molar ratio of 3-aminophenol to silica decreases, uniform pores with the size corresponding to the silica nanoparticles (*i.e.* ~ 13 nm) are observed in Figure 3(e) although there are still many mesopores with

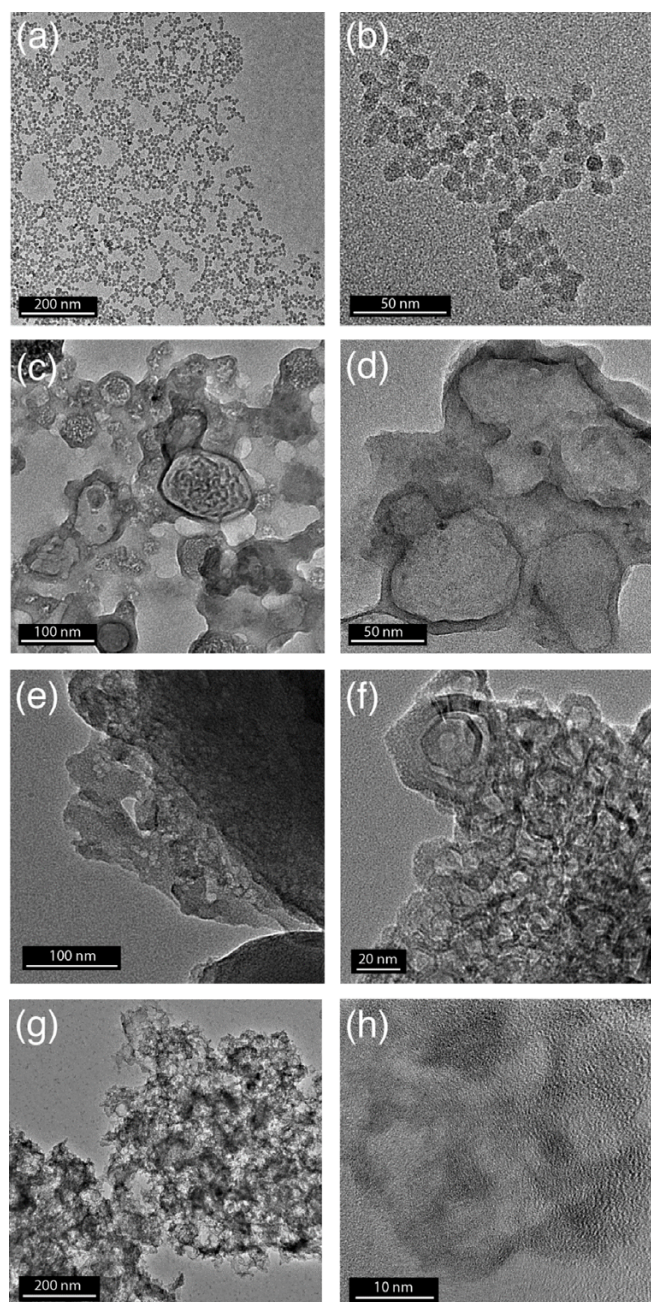


Figure 3. Transmission electron micrographs at low and high magnification of (a, b) neat silica nanoparticles ($d \sim 13$ nm), (c, d) PoC-1 (1:5), (e, f) PoC-2 (1:10), and (g, h) PoC-3 (1:50) prepared by different ratios of 3-aminophenol to silica, respectively.

larger pore sizes (Figure 3(f)). More significant changes in the morphology of porous carbon networks occur at the lowest molar ratio (1:50) as depicted in Figure 3(g) and 3(h). In particular, Figure 3(g) reveals a development of porous carbon network, in which magnified image (Figure 3(h)) highlights the detailed morphologies of nanosphere-interconnected structures.

To evaluate the microstructure of the pores depending on the molar ratio of 3-aminophenol to silica, the N₂ adsorption-desorption isotherms and the corresponding pore size distribution of porous carbon networks are obtained as shown in Figure 4. The hysteresis at the high pressure of N₂ adsorption-desorption isotherms of all these carbon materials strongly

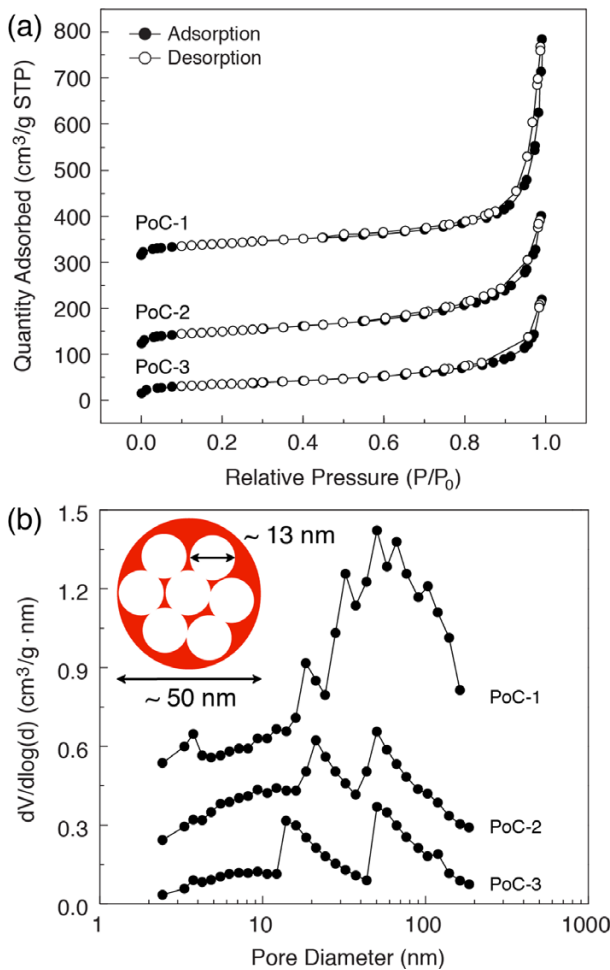


Figure 4. (a) N_2 adsorption-desorption isotherm and (b) the corresponding pore size distribution of the sample PoC-1, PoC-2, and PoC-3. Each curve is shifted successively to enhance clarity of the graphic.

suggests the presence of mesopores (Figure 4(a)). The pore size distribution of PoC-1 was quite broad in the ranges of 20~200 nm, consistent with the electron micrographs in Figure 3(c) and 3(d). This result indicates that 3-AF resin gels are formed around the silica aggregates in basic condition of pH ~8 by adding ammonia solution, however, they do not seem to fill the interstitial regions between the individual silica nanoparticles since a pore size distribution corresponding to the size of

silica nanoparticles is not observed in case of PoC-1 (Figure 4(b)). Such a broad pore size distribution arising from uncontrolled coating of 3-AF resins onto the aggregates is consistent with the previous results observed in similar systems except using resorcinol-formaldehyde instead of 3-aminophenol-formaldehyde.¹⁸

Interestingly, a bimodal pore size distribution appears when the concentration of 3-AF resins decreases to 1:10 for PoC-2 with larger pores of ~50 nm and smaller pores (~21 nm). In particular, the size of smaller pores further decreased to 14 nm (PoC-3) corresponding to that of silica nanoparticles while larger pores exhibit similar pore size distribution (*i.e.* 50~100 nm). This indicates that relatively low concentrations of 3-aminophenol and formaldehyde effectively form a more uniform 3-AF layer on the surface of each silica nanoparticle consisting of aggregates, resulting in the nanosphere-interconnected carbon networks as illustrated in the inset of Figure 4(b). Low and high magnification TEM image in Figure 3(g) and 3(h), confirms that the nanospheres are 3-dimensionally interconnected with each other in carbon networks, resulting in the bimodal pore size distribution arising from the each nanospheres (*i.e.* smaller pores ~13 nm) and interconnected nanospheres (*i.e.* larger pores ~50 nm) originated from the aggregates, respectively.

Due to the hydroxyl groups on the surface of SiO_2 in the ethanol/water mixture, 3-aminophenol would form an adsorbed layer on their surface via hydrogen bonding between amino (-NH₂) and hydroxyl (-OH) groups of 3-aminophenol and SiO_2 , respectively.²¹ Upon the addition of formaldehyde into the solution, 3-aminophenol, formaldehyde, and ammonia react to form the mixtures of addition and condensation compounds such as hydroxymethyl and benzoxazine derivatives, resulting in the 3-AF resin/ SiO_2 core-shell structures.^{15,22-25} Here, we need to note that careful control of 3-aminophenol amounts on SiO_2 plays a crucial role to determine the microstructure of 3-AF resin/ SiO_2 (*i.e.* porous carbon materials) since an excess of external 3-aminophenol in the mixture would be able to react with formaldehyde and produce uncontrolled structures of 3-AF in the absence of SiO_2 templates. Also, an amine group (-NH₂) of 3-aminophenol would be more effective to form the phenol layer around SiO_2 , compared to resorcinol with two hydroxyl groups (-OH), which is uniquely distinguished from the other ones by means of various templates. Therefore, these results clearly

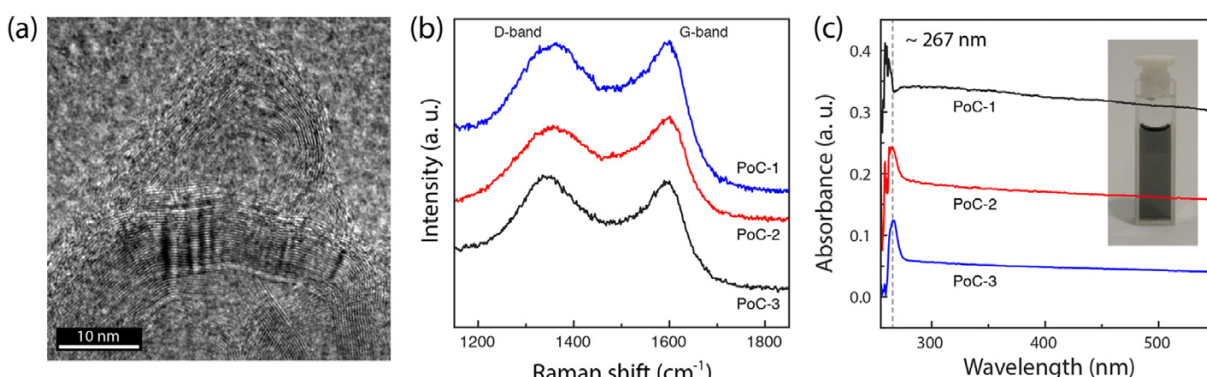


Figure 5. (a) Transmission electron image depicting the hollow carbon nanoparticles. (b) Raman spectra and (c) the corresponding optical absorbance of the PoC-1, PoC-2, PoC-3, respectively. Each curve is shifted successively to enhance clarity of the graphic.

demonstrate that the uniform 3-AF resin coating at lower molar concentrations form the hierarchical nanostructure of nanosphere-interconnected carbon networks.

A formation of carbon layers consisting of about five to eight graphene layers in the nanosphere-interconnected networks (Figure 5(a)) reveals a development of uniform and dense nanographene islands with a mixed amorphous and polycrystalline nature. In order to confirm the growth of crystalline graphene, Raman spectroscopy was employed for PoC-1, PoC-2, and PoC-3. Figure 5(b) exhibits broad peaks occurred around 1360 (D band due to breathing modes of sp^2 carbon atoms in rings) and 1580 cm^{-1} (G band arising from the graphitic carbon phase with the bond stretching between pairs of sp^2 carbon atoms).^{26,27} The reduced D-to-G band peak intensity ratio (I_D/I_G) of ~ 0.9 suggests that they possess relatively higher degree of graphite structures. This is also confirmed by the optoelectronic properties of PoC-1, PoC-2, and PoC-3 arising from the π states of the sp^2 sites, in which the main absorbance peak attributed to $\pi\text{-}\pi^*$ transitions of C=C in the reduced graphene oxide occurs at around ~ 260 nm whereas no shoulder peaks at ~ 300 nm, attributed to $n\text{-}\pi^*$ transitions of C=O (Figure 4(c)).²⁸

4. Conclusions

In conclusion, porous carbon networks with a nanosphere-interconnected structure were successfully synthesized via 3-aminophenol and formaldehyde polymerization in the presence of silica nanoparticles, followed by carbonization. Systematic investigation of the ratio of carbon precursors and silica nanoparticles showed that the microstructure of porous carbon materials was closely related to their preferential distribution onto the surface of silica nanoparticles, yielding structurally controlled hybrid nanoparticles with a SiO_2 core and a shell of variable thickness composed of well-defined 3-AF resins. Formation of nanosphere-interconnected network at lower concentration of 3-aminophenol to silica clearly showed the bimodal pore size distribution with a high degree of structural order and more wide controllability, compared to the resorcinol and formaldehyde resins, which is associated with the hollow carbon nanospheres corresponding to the size of SiO_2 cores (~ 13 nm) and their aggregates ($\sim 50\text{-}100$ nm). Fine control of the nanostructure in the carbon materials can open up new opportunities for high-performance nanoscale applications that require an efficient fabrication method for preparation of the mesoporous carbon networks.

References

- (1) M. Oh and C. A. Mirkin, *Nature*, **438**, 651 (2005).
- (2) A. Nieto-Márquez, R. Romero, A. Romero, and J. L. Valverde, *J. Mater. Chem.*, **21**, 1664 (2011).
- (3) A. D. Roberts, X. Li, and H. Zhang, *Chem. Soc. Rev.*, **43**, 4341 (2014).
- (4) J. Liu, N. P. Wickramaratne, S. Z. Qiao, and M. Jaroniec, *Nat. Mater.*, **14**, 763 (2015).
- (5) J. Lee, J. Kim, and T. Hyeon, *Adv. Mater.*, **18**, 2073 (2006).
- (6) R. J. White, K. Tauer, M. Antonietti, and M.-M. Titirici, *J. Am. Chem. Soc.*, **132**, 17360 (2010).
- (7) Z. Li, D. Wu, Y. Liang, R. Fu, and K. Matyjaszewski, *J. Am. Chem. Soc.*, **136**, 4805 (2014).
- (8) D. Wu, C. M. Hui, H. Dong, J. Pietrasik, H. J. Ryu, Z. Li, M. Zhong, H. He, E. K. Kim, M. Jaroniec, T. Kowalewski, and K. Matyjaszewski, *Macromolecules*, **44**, 5846 (2011).
- (9) J. Schuster, G. He, B. Mandlmeier, T. Yim, K. T. Lee, T. Bein, and L. F. Nazar, *Angew. Chem. Int. Ed.*, **51**, 3591 (2012).
- (10) J. Liu, T. Yang, D.-W. Wang, G. Q. Lu, D. Zhao, and S. Z. Qiao, *Nat. Commun.*, **4**, 2798 (2013).
- (11) D. Kim, A. Kirakosyan, and J. Choi, *Macromol. Rapid Commun.*, **37**, 1507 (2016).
- (12) N. P. Wickramaratne and M. Jaroniec, *J. Mater. Chem. A*, **1**, 112 (2013).
- (13) Y. Liang, R. Fu, and D. Wu, *ACS Nano*, **7**, 1748 (2013).
- (14) Z. Chi, W. Zhang, X. Wang, F. Cheng, J. Chen, A. Cao, and L. Wan, *ACS Appl. Mater. Interfaces*, **6**, 22719 (2014).
- (15) R. W. Pekala, *J. Mater. Sci.*, **24**, 3221 (1989).
- (16) J. Liu, S. Z. Qiao, H. Liu, J. Chen, A. Orpe, D. Zhao, and G. Q. Lu, *Angew. Chem. Int. Ed.*, **50**, 5947 (2011).
- (17) T. Liu, L. Qu, K. Qian, J. Liu, Q. Zhang, L. Liu, and S. Liu, *Chem. Commun.*, **52**, 1709 (2016).
- (18) S. Han, K. Sohn, and T. Hyeon, *Chem. Mater.*, **12**, 3337 (2000).
- (19) J. Zhao, W. Niu, L. Zhang, H. Cai, M. Han, Y. Yuan, S. Majeed, S. Anjum, and G. Xu, *Macromolecules*, **46**, 140 (2013).
- (20) J. Zhao, R. Luque, W. Qi, J. Lai, W. Gao, M. R. H. S. Gilani, and G. Xu, *J. Mater. Chem. A*, **3**, 519 (2015).
- (21) C. Lin and J. A. Ritter, *Carbon*, **35**, 1271 (1997).
- (22) S. Wang, W.-C. Li, G.-P. Hao, Y. Hao, Q. Sun, X.-Q. Zhang, A.-H. Lu, *J. Am. Chem. Soc.*, **133**, 15304 (2011).
- (23) A. Pizzi, R. Garcia, and S. Wang, *J. Appl. Polym. Sci.*, **66**, 255 (1997).
- (24) D.-D. Guo, M.-S. Zhan, and K. Wang, *J. Appl. Polym. Sci.*, **126**, 2010 (2012).
- (25) C. P. R. Nair, *Prog. Polym. Sci.*, **29**, 401 (2004).
- (26) A. C. Ferrari and J. Robertson, *Phys. Rev. B*, **61**, 14095 (2000).
- (27) A. C. Ferrari, *Solid State Commun.*, **143**, 47 (2007).
- (28) P. V. Kumar, N. M. Bardhan, S. Tongay, J. Wu, A. M. Belcher, and J. C. Grossman, *Nat. Chem.*, **6**, 151 (2014).